

NJC

Accepted Manuscript



This is an *Accepted Manuscript*, which has been through the Royal Society of Chemistry peer review process and has been accepted for publication.

Accepted Manuscripts are published online shortly after acceptance, before technical editing, formatting and proof reading. Using this free service, authors can make their results available to the community, in citable form, before we publish the edited article. We will replace this *Accepted Manuscript* with the edited and formatted *Advance Article* as soon as it is available.

You can find more information about *Accepted Manuscripts* in the [Information for Authors](#).

Please note that technical editing may introduce minor changes to the text and/or graphics, which may alter content. The journal's standard [Terms & Conditions](#) and the [Ethical guidelines](#) still apply. In no event shall the Royal Society of Chemistry be held responsible for any errors or omissions in this *Accepted Manuscript* or any consequences arising from the use of any information it contains.

Quantum Monte Carlo study on electron correlation effects in small aluminum hydride clusters

J. Higino Damasceno Jr.*[†] J.N. Teixeira Rabelo[‡] Ladir Cândido[§]

January 8, 2015

Abstract

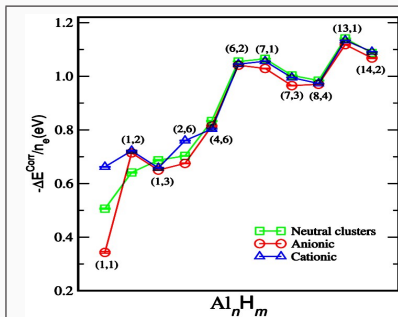
Using fixed-node diffusion quantum Monte Carlo (DMC) method, we investigate the electron correlation in several small relaxed and unrelaxed neutral, cationic, and anionic aluminum hydride clusters. We calculate the clusters total energies and use them to obtain the binding energies. Our results are in very good agreement with available *ab-initio* calculations and anion-photoelectron spectroscopy experiments. The calculations are also performed in the Hartree-Fock (HF) approximation in order to analyse the impact of electron correlation. For the total atomic binding energy, i.e. the energy necessary to separate all the atoms, this impact varies from 20% up to about 50%, whereas for the electron binding energy, i.e. the required energy to detach or attach an electron to the cluster, it ranges from 1% up to 73%. The decomposition of the electron binding energies clearly shows that both charge redistribution and electron correlation are important in determining the detachment energies, whereas electrostatic and exchange interactions are responsible for the ionization potential.

*Coordenação de Física, Universidade Federal de Goiás - UFG, Campus Jataí BR 364, Km 192, 75801-615, Jataí, Goiás, Brazil.

[†]Instituto de Física, Universidade Federal de Goiás - UFG, 74001-970, Goiânia, Go, Brazil

[‡]Instituto de Física, Universidade Federal de Goiás - UFG, 74001-970, Goiânia, Go, Brazil

[§]Instituto de Física, Universidade Federal de Goiás - UFG, 74001-970, Goiânia, Go, Brazil



Using accurate methods we calculate binding energies to discuss the electron-electron interaction in the formation of $Al_n H_m$ ionic clusters.

1 Introduction

Aluminum hydride clusters, Al_nH_m , are currently attracting great interest as highly promising efficient hydrogen storage systems with large impact on technological applications¹⁻³. A major issue in this respect is the energetics and stability of these clusters and their dependence on the number and charge distribution of hydrogen in the cluster formation. An important role here must be played by the electron correlation. It is critical for the accurate and quantitative evaluation of the clusters energies. Until recently, most of experimental using photoelectron spectroscopy and theoretical with density functional theory (DFT) works have been devoted mainly to the characterization of bonding and structure of several Al_nH_m ^{4-6,6-10,12-15}. The nature of their bonding and structure can in principle be characterized by two regimes: for $n \gg m$ the system is rich in free electrons and may be understood in terms of a jellium model^{10,16}; otherwise, for $n \ll m$ the electrons are more localized favoring the covalent bond, a regime not yet well understood. For certain numbers of valence electrons they are very stable, have low electron affinity, high ionization potential, and are known as "magic clusters"¹⁷⁻²¹.

Although DFT is the most widely used theoretical method, it faces challenges to achieve chemical accuracy in the predictions of physical quantities²². Hence, the use of more accurate methods to properly treat the electron correlation is of relevance to a better understanding of the physics of aluminum hydride clusters as well as of the metallic clusters in general. The coupled cluster (CC) and full configuration interaction (FCI) methods are more accurate than DFT. Quantum Monte Carlo method (QMC) can achieve accuracy similar to such methods, with the advantage of provide estimates of statistical errors in quantum calculations²³⁻²⁶.

In this work, we perform QMC simulation for a quantitative study of several selected aluminum hydride clusters in their neutral and charged states. The smallest ones have been chosen in order to understand the effects of addition of hydrogen to the system, while the largest ones because they show a very large HOMO-LUMO gap and are very populated in spectroscopic experiments, besides the possible technological proposals. Accurate Hartree-Fock (HF) and fixed-node diffusion quantum Monte Carlo (DMC) evaluations of the ground state energy enable us to analyse the contribution of correlation to the atomic and electronic

binding energies. The set of data provided here can be of interest for those working on the development of quantum chemistry approaches with possible applications to metallic clusters in general, and to hydrogen storage problems in particular. Furthermore, the decomposition of the electron binding energy into electrostatic, relaxation, and correlation energies and an analysis of their contributions allow us to better understand the mechanism of formation of the cationic and anionic clusters.

2 Methodology and computational details

The QMC calculations reported here are carried out within the variational (VMC) and fixed-node diffusion (DMC) quantum Monte Carlo methods using the CASINO code²⁷. The VMC/DMC methods are well documented in the literature^{24,28}. Therefore, we shall give here only the main computational details of the simulation.

The VMC trial wave functions are of the Slater-Jastrow type

$$\psi_T(\mathbf{R}) = D_{\uparrow}(\phi_i)D_{\downarrow}(\phi_i)e^U, \quad (1)$$

where $D_{\uparrow\downarrow}$ are the determinants of up and down spin orbitals, ϕ 's are the single-particle orbitals obtained from DFT single-point calculations with a gaussian basis set 6-311++G(2d,2p) obtained from EMSL (Basis set exchange library)²⁹, as implemented in the Gaussian code³⁰, using the BPW91 exchange correlation functional. For the Jastrow factor, U in Eq. (1), we use one that has been developed by Drummond-Towler-Needs³¹ as implemented in the CASINO code with two terms, $u(\mathbf{r}_{ij}, \alpha)$ and $\chi(\mathbf{r}_{iI}, \beta)$, namely the electron-electron and electron-nucleous terms respectively,

$$U(\mathbf{r}_i, \mathbf{r}_I; \alpha, \beta) = \sum_i^{N-1} \sum_{j=i+1}^N u(\mathbf{r}_{ij}, \alpha) + \sum_{I=1}^{N_{cores}} \sum_{i=1}^N \chi(\mathbf{r}_{iI}, \beta). \quad (2)$$

Here, u and χ are represented by power expansions; N is the number of electrons and N_{cores} the number of cores, $\mathbf{r}_{ij} = \mathbf{r}_i - \mathbf{r}_j$, $\mathbf{r}_{iI} = \mathbf{r}_i - \mathbf{r}_I$, \mathbf{r}_i and \mathbf{r}_I being the electron and core positions respectively; α and β are variational parameters which are optimized for every structure by the method of variance minimization³²⁻³⁴. The Dirac-Fock average relativistic effective potential (AREP)^{35,36} is used to represent the core electrons. The core polarization

correction is added to the pseudopotential to account for core-electron correlation. Hence, the calculations go beyond the frozen core approximation³⁷. We then employ the optimized trial VMC wavefunction as a guide one for the importance sampling in the DMC method²⁴. We use the fixed node approximation (FN) which assumes the nodes of the DMC solution (the nodes of ψ_0) to be the same nodes of the trial wave function, ψ_T ^{38,39}. For the fixed-node DMC simulation, we use a time-step of 0.001 a.u. (we have evaluated the time step dependence of the total energy for a few systems, and found it to be negligible within the error bar) that produces for most of the calculation a very high acceptance ratio of more than 99.99%, and an ensemble of 10000 walkers. Checks with up to five times the number of walkers do not change the results within the statistical error. For the averages in the DMC calculations we consider about 1.0×10^6 QMC moves.

The Gaussian package³⁰ has also been used to evaluate the HF total energies with the same basis set used for the DFT calculations. Because most of the studied clusters are open shell systems, for which the number of electrons of each spin are not equal, we performed for those systems the unrestricted Hartree-Fock (UHF) calculations. However, we did not make distinctions between the restricted and unrestricted HF in the discussion of the results, we have called such calculations just HF. Checks of the total energies for small clusters in the infinitely large complete basis set show that the corrections are small and can be neglected in this study since they are about 0.01 eV, i.e., smaller than the chemical accuracy which is about 0.05 eV.

3 Results and discussion

Figure 1 shows the set of low-lying energy structures considered in our study. The optimized neutral geometries are obtained by fully relaxing geometries that have been previously determined^{10,11} using DFT-BPW91 as implemented in the Gaussian03 code³⁰. Next, we obtain the cationics and anionics by respectively removing and adding one electron and afterwards fully relaxing the structure. In order to confirm that those structures represent the lowest-energy minima on the corresponding potential energy surface, a few clusters have been considered and a large number of input geometries were optimized with different spin multiplicities. The

full optimization process reduced the number to several energetically favorable structures, and the obtained lowest-lying structures were in agreement with those which we have taken from the literature as initial input geometries. All the studied clusters have spin singlet or doublet.

Table 1 shows HF and DMC results for the ground state total energy of the set of structures presented above. We show also in this table the results for three unrelaxed geometries, the neutral cluster at the anionic, $\text{Al}_n\text{H}_m^{0,-}$, the cationic at the neutral, $\text{Al}_n\text{H}_m^{+,0}$, and the anionic at the neutral, $\text{Al}_n\text{H}_m^{-,0}$ structures. The first two are useful to the estimation of electron affinity and ionization potential that can be compared with experimental measurements, while the latter is used to calculate the HF relaxation energy contribution which is also very useful in the energy decomposition of such quantities. From this table we see that the obtained ground state energies decrease with the increasing of the cluster size in both HF and DMC methods, following the same trend. The total energy is considerably lower in the DMC in comparison to HF.

The correlation energy is defined as the difference between the energy in the HF approximation and the energy given by DMC, $\Delta E^{\text{corr}} = E^{\text{DMC}} - E^{\text{HF}}$. In Fig. 2 we show the correlation energy per electron, $\Delta E^{\text{corr}}/n_e$, where n_e is the number of electrons in the cluster. It indicates that systems with $n > m$ are less sensitive than $n < m$ to both the number of electrons and charge of the system. For $n > m$ the correlation energy per electron is close to 1.0 eV which is typical in the normal phase of metals⁴⁰.

In the following results, the total binding energies are computed as

$$E_{\text{BE}} = E(\text{Al}_n\text{H}_m) - nE(\text{Al}) - mE(\text{H}), \quad (3)$$

where $E(\text{Al}_n\text{H}_m)$ is the total energy of the cluster, $E(\text{Al})$ the energy of an atom of Al, $E(\text{H})$ the energy of an atom of H, and n and m are the numbers of aluminum and hydrogen atoms respectively. We calculate the binding energy of H to $E(\text{Al}_n\text{H}_m)$ as

$$E_{\text{BE}}^{\text{H}} = E(\text{Al}_n\text{H}_m) - E(\text{Al}_n) - mE(\text{H}). \quad (4)$$

$E(\text{Al}_n)$ is the energy of the aluminum cluster considered rigid as it is in the cluster. The binding energy of Al to $E(\text{Al}_n\text{H}_m)$ is calculated as the difference between the Eqs. (3) and (4).

Table 1: Total energies calculated by HF and DMC for the relaxed clusters Al_n , Al_nH_m^0 , Al_nH_m^- and Al_nH_m^+ ; and for the unrelaxed clusters: $\text{Al}_n\text{H}_m^{0,-}$ (neutral cluster in the anionic geometry: $\text{Al}_n\text{H}_m^- - 1$ electron), $\text{Al}_n\text{H}_m^{+,0}$ (cationic cluster in the neutral cluster geometry: $\text{Al}_n\text{H}_m^0 - 1$ electron), and $\text{Al}_n\text{H}_m^{-,0}$ (anionic cluster in the neutral geometry: $\text{Al}_n\text{H}_m^0 + 1$ electron). All values are in eV units. Estimated statistical errors in the last decimal places are indicated in the parentheses.

Method (n, m)	Al_nH_m	Relaxed structure			Unrelaxed structure				
	Al_n	Al_nH_m^0	Al_nH_m^-	Al_nH_m^+	$\text{Al}_n\text{H}_m^{0,-}$	$\text{Al}_n\text{H}_m^{+,0}$	$\text{Al}_n\text{H}_m^{-,0}$		
HF	1, 1	-51.113	-66.979	-66.751	-59.755	-66.960	-59.722	-66.756	
	1, 2		-82.642	-82.612	-75.896	-82.193	-74.914	-82.348	
	1, 3		-99.191	-98.074	-89.406	-98.544	-88.535	-98.859	
	2, 6	-101.605	-199.664	-199.724	-188.614	-197.582	-188.499	-198.505	
	4, 6	-206.437	-304.107	-304.763	-297.554	-303.889	-296.773	-304.659	
	6, 2	-311.208	-342.815	-344.580	-337.062	-342.614	-336.675	-344.042	
	7, 1	-364.661	-380.901	-382.457	-375.067	-380.599	-374.868	-382.180	
	7, 3		-412.830	-414.580	-406.971	-412.566	-406.778	-414.318	
	8, 4	-416.059	-482.144	-483.523	-476.563	-481.687	-476.484	-483.210	
	13, 1	-679.095	-695.016	-696.847	-689.696	-694.828	-688.953	-696.646	
	14, 2	-731.912	-764.754	-766.819	-759.143	-764.517	-758.610	-766.686	
	DMC	1, 1	-53.214(7)	-70.012(8)	-70.18(1)	-61.741(5)	-69.97(1)	-61.673(6)	
		1, 2		-85.85(1)	-86.90(1)	-78.78(1)	-85.43(2)	-77.91(1)	
		1, 3		-103.31(1)	-103.63(1)	-92.70(1)	-102.71(1)	-91.73(1)	
2, 6		-107.34(2)	-208.10(1)	-208.50(1)	-196.97(1)	-206.11(1)	-196.90(1)		
4, 6		-218.42(2)	-319.11(1)	-320.24(2)	-311.20(2)	-318.84(1)	-310.64(2)		
6, 2		-330.92(1)	-363.92(2)	-365.44(2)	-356.92(1)	-363.85(2)	-356.89(2)		
7, 1		-387.43(2)	-404.33(1)	-406.13(2)	-397.25(1)	-403.98(2)	-397.13(2)		
7, 3			-436.90(2)	-438.71(2)	-429.86(2)	-436.63(2)	-429.80(2)		
8, 4		-442.78(2)	-509.73(2)	-511.66(2)	-502.82(2)	-509.69(2)	-502.82(2)		
13, 1		-724.31(9)	-740.64(2)	-742.67(3)	-733.91(2)	-740.33(2)	-733.77(3)		
14, 2		-780.59(9)	-813.66(3)	-815.96(7)	-807.14(1)	-813.41(4)	-806.51(3)		

Table 2: Binding energies (BE's) of several selected neutral Al_nH_m clusters using HF, DMC and *ab initio* plane wave method (PWM)²⁰. Statistical errors in the last decimal place are indicated in parenthesis. All energies are in eV units.

Method	Al_nH_m (n, m)	E_{BE}	$E_{\text{BE}}^{\text{Al}}$	E_{BE}^{H}
HF	1,1	-2.26	-	-2.26
	1,2	-4.32	-	-4.32
	1,3	-7.26	-	-7.26
	2,6	-15.81	0.62	-16.43
	4,6	-18.03	-1.99	-16.04
	6,2	-8.93	-4.53	-4.40
	7,1	-9.51	-6.87	-2.63
	7,3	-14.23	-6.87	-7.35
	8,4	-18.82	-7.16	-11.67
	13,1	-16.95	-14.63	-2.32
	14,2	-21.97	-16.34	-5.63
DMC	1,1	-3.19(1)	-	-3.19(1)
	1,2	-5.42(1)	-	-5.42(1)
	1,3	-9.28(1)	-	-9.28(1)
	2,6	-20.04(2)	-0.91(2)	-19.13(2)
	4,6	-24.62(2)	-5.56(2)	-19.06(2)
	6,2	-17.43(2)	-11.63(2)	-5.79(2)
	7,1	-18.23(2)	-14.93(5)	-3.29(2)
	7,3	-23.59(3)	-14.94(4)	-8.65(3)
	8,4	-29.56(3)	-17.07(3)	-12.49(3)
	13,1	-35.25(3)	-32.53(9)	-2.73(9)
14,2	-41.46(4)	-35.6(1)	-5.86(9)	
PWM	1,1	-3.150	-	-3.150
	1,2	-5.405	-	-5.405
	6,2	-18.761	-	-5.898
	7,1	-19.612	-	-3.177
	13,1	-27.866	-	-3.020

Table 2 shows the decomposition of the total binding energy (BE) (third column) in the BE of Al (fourth column) and of H (fifth column). The HF and DMC total BE of the neutral clusters increase negatively with increasing cluster size following the same trend observed in a previous study that used *ab-initio* plane wave methods²⁰. Note that, the absence of electron correlation in the cluster Al_2H_6 makes the aluminum atoms in the cluster unbound. The DMC binding energies of the hydrogen atoms are about 3 eV per atom whereas for the aluminum it increases slowly with the number of atoms, for the largest cluster the binding energy per atom is about 2.5 eV.

In Table 3 we present the electron correlation contribution to the total BE and BE of hydrogen and aluminum defined as the difference between the binding energies (given by the

Table 3: Electron correlation contribution to BE of the Al_nH_m clusters. The digits in parentheses are estimated statistical error in the last decimal place. The energies are in eV units.

Al_nH_m (n, m)	E_{BE}	$E_{\text{BE}}^{\text{Al}}$	E_{BE}^{H}
1,1	-0.93(1)	-	-0.93(1)
1,2	-1.12(1)	-	-1.12(1)
1,3	-2.02(1)	-	-2.02(1)
2,6	-4.23(2)	-1.53(2)	-2.70(2)
4,6	-6.59(3)	-3.58(2)	-3.02(2)
6,2	-8.49(4)	-7.10(4)	-1.39(2)
7,1	-8.72(5)	-8.06(5)	-0.66(3)
7,3	-9.36(5)	-8.06(5)	-1.30(3)
8,4	-10.73(6)	-9.91(6)	-0.82(3)
13,1	-18.31(9)	-17.9(1)	-0.41(9)
14,2	-19.5(1)	-19.3(1)	-0.23(9)

Eq. (3)) obtained by DMC and HF. The estimates of the relevance of the correlation energy in the total BE show that the electron correlation contribution varies from about 20% to 50%. It is interesting to observe that AlH_3 is supposedly one of the most stable structures though it does not have the higher correlation energy contribution, which is about 22%, amongst all studied clusters. Therefore, it seems that the correlation effects on the atomic BE are not decisive to the choice of the most stable cluster. For $n < m$, the BE of H dominates while for $n > m$ it is the BE of Al that has the largest contribution.

Next, we compare our results with some measurable quantities like the adiabatic ionization potential (AIP), computed as

$$\text{AIP} = E^+ - E^0, \quad (5)$$

where E^0 and E^+ are total energies of the neutral and cationic clusters, and the vertical

ionization potential (VIP), given by

$$\text{VIP} = E^{+,0} - E^0, \quad (6)$$

where $E^{+,0}$ is the total energy of the cationic in the neutral geometry. We also compute the adiabatic electron detachment energy (ADE) as

$$\text{ADE} = E^0 - E^-, \quad (7)$$

where E^- is the total energy of the the anionic cluster, and the vertical electron detachment energy (VDE) by the following formula

$$\text{VDE} = E^{0,-} - E^-, \quad (8)$$

where $E^{0,-}$ is the neutral cluster energy in the anionic structure.

Table 4: Basis set dependence of the ADE in the CCSD(T) and fixed-node DMC calculations for AlH_2 . The numbers in parentheses are estimated statistical error in the last decimal place. All energies are in eV.

Basis Set	CCSD(T)	DMC
6-31G	0.3283	1.0041(6)
6-311G	0.4835	1.0421(4)
6-311++G	0.7419	1.0449(4)
6-311++G(2d,2p)	0.9048	1.0367(4)
6-311++G(3d,3p)	0.9564	1.0286(4)
6-311++G(3df,3pd)	0.9946	1.0068(4)
aug-cc-pvtz	1.0394	1.0449(7)
aug-cc-pvqz	1.0426	1.0476(9)

In Table 4 we present the electron ADE of AlH_2 computed with different basis sets in the geometry given in Fig. 1 within the CCSD(T) and DMC methods. Results are presented for eight basis sets in order of increasing quality showing good convergence. The DMC is much less sensitive to the basis set size than CCSD(T) since the many-body DMC wave function is represented by the distribution of an ensemble of electrons and the basis set is used just

to expand the guide wave function that is required for the importance sampling^{39,41}. Note that, the agreement between them occurs only when the basis set of the CCSD(T) reaches the convergence. In the following calculations, we use the aug-cc-pvtz basis set for CCSD(T) due to both computer time and storage requirements.

Because of the small energy scales under consideration, we validate the DMC accuracy: (i) by comparing our results of ADE and VDE with those from CCSD(T) for the smallest four clusters, and (ii) with available experimental measurements of ADE and VDE using photo-electron spectroscopy^{4,6,10,12,14,15}. Table 5 shows HF and DMC results for ADE, VDE, VIP and AIP. Overall, the energies ADE and AIP are always smaller than VDE and VIP respectively. The differences between them for the HF case are an indication of structural relaxation of the neutral and cationic clusters for the detachment and ionization potential energies respectively. Also, in the absence of electron correlation (HF calculations), AlH, AlH₃, AlH₂ and Al₂H₆, draw attention because of: (i) negative sign values for AlH, AlH₂ and AlH₃; (ii) very small values of ADE and VDE for Al₂H₆; (iii) large difference between ADE and VDE for Al₂H₆. The negative values of ADE mean that the neutral cluster energy has lower value than the anionic's whereas for VDE it is the neutral cluster in the anionic structure that has lower value than anionic's. This happens because in the HF approximation the electron added to form the anionic cluster can not bind to this system, i.e., the addition of one electron to the neutral raises the total energy since the contribution of the (virtual) orbital of the added electron is positive. The ADE for Al₂H₆ is very small, and one possible reason for this is that the structures of the neutral and neutral at the anionic geometry clusters are very close to the anionic's. However, one can see that this is not the case since as shown in Fig. 1 the aforementioned structures are very different. Thus, the attached electron to the neutral to form the anionic cluster changes significantly the anionic structure. Therefore, a considerable change in the electronic configuration of these clusters could be the reason why such systems have energies so close that ADE and VDE are so small. The huge difference between ADE and VDE for Al₂H₆ means that this cluster must have the largest structural relaxation contribution energy amongst all the others.

The role played by the electron correlation is prominent and can be seen by looking at the DMC data, i.e., the HF behavior (negative values) for ADE and VDE of AlH, AlH₂ and

AlH₃ has been corrected by the inclusion of the valence electron correlation. Both HF and DMC follow the same trend, i.e. the vertical energies are larger than the adiabatic ones. The largest differences between VDE and ADE are for AlH₃ and Al₂H₆, for which VDE is about three and six times larger than ADE respectively. It is also clear that in general the correlation increases the electron binding energies.

We add also to Table 5 related previous theoretical and experimental data. As one can see, the DMC results are found to be fairly close to the experimental values within a discrepancy smaller than a few percents. Our worst result, which is for Al₁₄H₂, has a discrepancy of 4% with experiment without taking into account the errors, and considering the errors (i.e. 2.30 ± 0.07 of the DMC VDE against the experimental result 2.4 ± 0.1 eV), the lower bound of experimental VDE is 2.3 eV and the upper bound of the DMC values is 2.37 eV. This difference is 0.07 eV which corresponds to less than 2.5% of the VDE values. Therefore, the DMC energies reported here can be considered to be very accurate and can be used to access the accuracy of other theoretical approaches. Thus, comparing the obtained results with DFT for VIP we see a qualitative agreement with those of Rao *et al.*¹⁴. Quantitatively, their VIP results are overestimated for AlH₂ in about 1.3 eV, and underestimated for AlH₃ and Al₂H₆ in about 0.15 and 1.0 eV respectively. The ADE and VDE results are in good agreement with the energies of Kiran *et al.*¹⁰ the differences being smaller or about 0.1 eV. This is consistent with our previous QMC study for small aluminum clusters²⁶.

In order to study the effects of attaching and detaching an electron to Al_nH_m, we decompose each of the electron binding energies, Eqs. (5-8), into three components as follows

$$\Delta E^e = \Delta E_{\text{HF}}^{ex} + \Delta E_{\text{HF}}^{\text{relax}} + \Delta E_e^{\text{corr}}. \quad (9)$$

Here, we separate the HF energies in $\Delta E_{\text{HF}}^{ex}$, which takes into account only electrostatic and exchange interactions, and in the remainder energy $\Delta E_{\text{HF}}^{\text{relax}}$, which is the relaxation energy that takes into account the orbital relaxation or charge redistribution effects (even for vertical detachment energies and ionization potentials), and also the geometrical relaxation. The term ΔE_e^{corr} is the correlation energy that is calculated as $\Delta E_e^{\text{corr}} = \Delta E_{\text{DMC}}^e - \Delta E_{\text{HF}}^e$.

For the electron affinity, we have $\Delta E_{\text{HF}}^{ex} = E_{\text{HF}}^0 - E_{\text{HF}}^{-,0}$, in which both energies are calculated for the neutral geometry, and $\Delta E_{\text{HF}}^{\text{relax}} = E_{\text{HF}}^{-,0} - E_{\text{HF}}^-$, whereas the energy correlation for ADE

Table 5: The AIP, VIP, ADE and VDE energies for several Al_nH_m using HF and DMC. Results for CCSD(T), available DFT^{9,10,14}, and experimental measurement^{4,6,10,12,14,15} are also given for comparison. All values are in eV units. Estimated statistical errors in the last decimal places are indicated in the parentheses.

Method	Al_nH_m (n, m)	AIP	VIP	ADE	VDE	
HF	1, 1	7.22	7.25	-0.23	-0.21	
	1, 2	6.75	7.73	-0.03	0.42	
	1, 3	9.78	10.66	-0.12	-0.53	
	2, 6	11.05	11.16	0.06	2.14	
	4, 6	6.55	7.33	0.66	0.87	
	6, 2	5.75	6.14	0.76	0.97	
	7, 1	5.83	6.03	1.56	1.86	
	7, 3	5.86	6.05	1.75	2.01	
	8, 4	5.58	5.66	1.38	1.84	
	13, 1	5.32	6.06	1.83	2.02	
	14, 2	5.61	6.14	2.07	2.30	
	DMC	1, 1	8.27(1)	8.34(1)	0.17(1)	0.21(2)
		1, 2	7.06(1)	7.94(1)	1.05(1)	1.47(2)
		1, 3	10.61(2)	11.58(1)	0.32(1)	0.92(1)
2, 6		11.13(2)	11.20(2)	0.40(2)	2.39(2)	
4, 6		7.91(2)	8.47(3)	1.13(2)	1.40(2)	
6, 2		7.00(2)	7.02(2)	1.53(3)	1.60(3)	
7, 1		7.08(2)	7.20(2)	1.81(3)	2.15(3)	
7, 3		7.03(3)	7.10(3)	1.81(3)	2.08(3)	
8, 4		6.87(3)	6.87(3)	1.93(3)	1.97(3)	
13, 1		6.74(3)	6.87(4)	2.03(4)	2.34(4)	
14, 2		6.52(3)	7.16(4)	2.30(7)	2.55(8)	
CCSD(T)		1, 1			0.179	0.193
		1, 2			1.039	1.406
		1, 3			0.314	0.974
	2, 6			0.321	2.417	
DFT	1, 1		8.15	0.18		
	1, 2		7.92	0.9		
	1, 3		11.43	0.28		
	2, 6		10.14	0.44	2.42	
	4, 6			1.36	1.48	
	6, 2				1.76	
	7, 1			1.88	1.88	
	7, 3				2.01	
	8, 4			1.93	1.93	
	13, 1				1.99	
	14, 2			2.34	2.34	
	Expt.	1, 2			$\sim 0.9(1)$	$\sim 1.5(1)$
		1, 3			$\sim 0.3(1)$	$\sim 0.9(1)$
		2, 6				2.40(15)
4, 6				1.25(15)	1.35(5)	
6, 2					1.66(15)	
7, 1				1.85(5)		
7, 3					2.0(2)	
8, 4				1.95(5)		
13, 1				2.00(5)	2.2(1)	
14, 2				2.4(1)		

and VDE are given by $\Delta E_{ADE}^{corr} = [E_{DMC}^0 - E_{DMC}^-] - [E_{HF}^0 - E_{HF}^-]$ and $\Delta E_{VDE}^{corr} = [E_{DMC}^{0,-} - E_{DMC}^-] - [E_{HF}^{0,-} - E_{HF}^-]$, respectively.

For the ionization potential, we have $\Delta E_{HF}^{ex} = E_{HF}^{+,0} - E_{HF}^0$, in which both energies are calculated for the neutral geometry, and $\Delta E_{HF}^{relax} = E_{HF}^+ - E_{HF}^{+,0}$, whereas the energy correlation for AIP and VIP are given by $\Delta E_{AIP}^{corr} = [E_{DMC}^+ - E_{DMC}^0] - [E_{HF}^+ - E_{HF}^0]$ and $\Delta E_{VIP}^{corr} = [E_{DMC}^{+,0} - E_{DMC}^0] - [E_{HF}^{+,0} - E_{HF}^0]$, respectively.

Table 6 shows the energy decomposition of ADE, VDE, AIP, and VIP in the ground state of the aluminum hydride clusters calculated using DMC. The magnitude of the decomposition components of VDE, ADE, VIP and AIP shows in general an oscillating pattern

Table 6: Decomposition of the VED, AED, VIP and AIP in the ground state of several selected Al_nH_m clusters. Statistical error in the last decimal place are indicated in the parenthesis. All energies are in eV units.

Al_nH_m (n, m)	ΔE_{ex}^{HF}	ΔE_{HF}^{relax}	ΔE_{ADE}^{corr}	ΔE_{VDE}^{corr}	ADE	VDE
Anion						
1,1	-0.22	-0.01	0.40(2)	0.44(2)	0.17(2)	0.21(2)
1,2	-0.29	0.26	1.08(1)	1.50(2)	1.05(1)	1.47(2)
1,3	-0.33	0.21	0.43(1)	1.04(1)	0.32(1)	0.92(2)
2,6	-1.16	1.22	0.34(2)	2.33(2)	0.40(2)	2.39(2)
4,6	0.55	0.10	0.47(2)	0.74(2)	1.13(2)	1.40(2)
6,2	1.23	-0.46	0.76(3)	0.83(3)	1.53(3)	1.60(3)
7,1	1.28	0.28	0.25(3)	0.60(3)	1.81(3)	2.15(3)
7,3	1.49	0.26	0.06(3)	0.33(3)	1.81(3)	2.08(3)
8,4	1.07	0.31	0.60(3)	0.55(3)	1.93(3)	1.98(3)
13,1	1.63	0.20	0.20(4)	0.50(4)	2.03(4)	2.34(4)
14,2	1.93	0.13	0.23(7)	0.49(8)	2.30(7)	2.55(8)
			ΔE_{AIP}^{corr}	ΔE_{VIP}^{corr}	AIP	VIP
Cation						
1,1	7.26	-0.03	1.05(1)	1.11(1)	8.27(1)	8.34(1)
1,2	7.73	-0.98	0.32(1)	1.20(1)	7.06(1)	7.94(1)
1,3	10.66	-0.87	0.83(2)	1.79(1)	10.61(2)	11.58(1)
2,6	11.16	-0.11	0.08(2)	0.15(2)	11.13(2)	11.20(2)
4,6	7.33	-0.78	1.35(2)	1.91(3)	7.91(2)	8.47(3)
6,2	6.14	-0.39	1.25(2)	1.27(2)	7.00(3)	7.02(2)
7,1	6.03	-0.20	1.24(2)	1.37(2)	7.08(3)	7.20(2)
7,3	6.05	-0.19	1.18(3)	1.24(3)	7.03(3)	7.10(3)
8,4	5.66	-0.08	1.28(3)	1.28(3)	6.87(3)	6.87(3)
13,1	6.06	-0.74	1.42(3)	1.55(4)	6.74(3)	6.87(4)
14,2	6.14	-0.53	0.91(3)	1.54(4)	6.52(3)	7.16(4)

with increasing cluster size. For $n > m$ the oscillations are quantitatively small in comparison with those for $n < m$. The results show that electron correlation is important for the stabilization of the clusters, especially for ADE and VDE when $n < m$, the contribution ranging from 3% up to 73%, VDE being impacted more. In the most stable cluster AlH_3^- , the dominant contribution is provided by the electron correlation which is about 65%. On the other hand, for $n > m$ the correlation energy still has some important contribution but with less impact and varies from about 3% to 33% with also a larger impact on VDE; however, the main contribution to VDE comes from the HF energies. For the ionization potential there occurs a change of scenario, i.e., now the HF energy, mainly electrostatic and exchange interactions, dominates the energy contributions of AIP and VIP for both regimes, $n < m$ and $n > m$. The relaxation energy and the electron correlation represent a smaller fraction of the ionization potential energy. The larger contribution of the electron correlation is of about 19% of VIP for Al_4H_6 , Al_{13}H and Al_{14}H_2 . This could be one of the reasons why the HF approximation gives good results for the ionization potential and poor descriptions for the electron affinities. Those results also show that the electrostatic and exchange interactions $\Delta E_{\text{HF}}^{\text{ex}}$, in general help to the stabilization of the Al_nH_m with excess or miss electron. For the four clusters with excess electron AlH^- , AlH_2^- , AlH_3^- , and Al_2H_6^- they play a destabilization role. Also, the relaxation energy contribution, $\Delta E_{\text{relax}}^{\text{HF}}$, plays a stabilization (destabilization) role for clusters with excess (miss) electron in Al_nH_m top (bottom) of Table 5. In general, the correlation energy, ΔE^{corr} , helps to stabilize most of the studied clusters.

4 Conclusion

We have carried out quantum Monte Carlo calculations of selected neutral and charged aluminum hydride clusters, and have evaluated the correlation energy of valence electrons on the atomic as well as on the electron binding energies AIP, VIP, ADE and VDE. The obtained results for VDE and ADE agree very well with available experimental data suggesting that the considered structures are very close to those populated in the experiment. Our findings show that the electron correlation on the total atomic binding energy has an impact that varies from 20% up to about 50%, whereas for the electron binding energy it ranges from 1%

up to 73%. Furthermore, the anionic AIH is stabilized exclusively by the electron correlation. The decomposition of AIP, VIP, ADE and VDE energies shows that the electrostatic and exchange interactions are the main responsible for the stabilization of the miss electron in the cationic clusters whereas for clusters with electron in excess both of the effects, the orbital relaxation (or charge redistribution) and the correlation energy, play an important role and must be treated properly in order to study anionic clusters.

5 ACKNOWLEDGMENTS

This research was supported by FAPEG and CNPq.

References

1. J. Graetz, J.J. Reilly, V.A. Yartys, J.P. Maehlen, B.M. Bylychev, V.E. Antonov, B.P. Tarasov and I.E. Gabis, *J. Alloys Compd.*, 2011, **509**, S517.
2. R. Zidan, B. L. Garcia-Dias, C.S. Fewox, A.C. Stowe, J.R. Gray, and A.G. Harter, *Chem. Commun.*, 2009, 3717.
3. M. Felderhoff, M.C. Weidenthaler, R. Von Helmot, and U. Eberle, *Phys. Chem. Chem. Phys.*, 2007, **9**, 2643.
4. X. Zhang, H. Wang, E. Collins, A. Lim, G. Gantefor, B. Kiran, H. Schnockel, B. Eichhorn and K. Bowen, *J. Chem. Phys.*, 2013, **138**, 124303.
5. K. Lian, Y. Jian, D. Fei, W. Feng, M. Jin, D. Ding and Y. Luo, *Chin. J. Chem. Phys.*, 2012, **25**, 147.
6. A. Grubisic, X. Li, S.T. Stokes, K. Vetter, G.F. Gantefor, K.H. Bowen, P. Jena, B. Kiran, R. Burgert and H. Schnockel, *J. Chem. Phys.*, 2009, **131**, 121103.
7. P. J. Roach, W.H. Woodward, A.W. Castleman Jr., A. C. Reber and S.N. khanna, *Science*, 2009, **323** 492.

8. P.J. Roach, A.C. Reber, W.H. Woodward, S.N. Khanna and A.W. Castleman, Jr., *Proc. Nat. Acad. Sci.*, 2007, **104**, 14565.
9. X. Li, A. Grubisic, S.T. Stokes, J. Cordes, G.F. Gantefor, K.H. Bowen, B. Kiran, M. Willis, P. Jena, R. Burget and H. Schnockel, *Science*, 2007, **315**, 356.
10. B. Kiran, P. Jena, X. Li, A. Grubisic, S.T. Stokes, G.F. Gantefor, K.H. Bowen, R. Burgert and H. Schnockel, *Phys. Rev. Lett.*, 2007, **98**, 256802.
11. J. Jung and Y.-K. Han, *Phys. Rev. Lett.*, 2008, **100**, 199701.
12. L-F. Cui, X. Li and L-S. Wang, *J. Chem. Phys.*, 2006, **124**, 054308.
13. J. Jung, Y-K Han, *J. Chem. Phys.*, 2006,**125**, 064306.
14. B.K. Rao, P. Jena, S. Burkart, G. Gantfor and G. Seifert, *Phys. Rev. Lett.*, 2001, **86**, 692.
15. S. Burkart, N. Blessing, B. Klipp, J. Muller, G. Gantefor and G. Seifert, *Chem. Phys. Lett.* 1999, **301** 546.
16. W. A. de Heer, *Rev. Mod. Phys.*, 1993, **65**, 611.
17. S. Saito and S. Ohnishi, *Phys. Rev. Lett.*, 1987, **59**, 190.
18. H. Hakkinen and M. Manninen, *Phys. Rev. Lett.*, **76**, 1599.
19. G. Rosenfeld, A.F. Becker, B. Poelsema, L.K. Verheij, and G. Comsa, *Phys. Rev. Lett.*, 1992, **69**, 917.
20. H. Kawamura, V. Kumar, Q. Sun and Y. Kawazoe, *Phys. Rev. B*, 2001, **65**, 045406.
21. S.N. Khanna and P. Jena, *Phys. Rev. Lett.*, 1992, **69**, 1664.
22. C.R. Hsing, P.L. Ríos, R.J. Needs and C.M. Wei, *Phys. Rev. B*, 2013, **88**, 165412.
23. A.J. Williamson, R. Q. Hood and J.C. Grossman, *Phys. Rev. Lett.*, 2001, **87** 246406.

24. W.M.C. Foulkes, L. Mitas, R.J. Needs and G. Rajagopal, *Rev. Mod. Phys.*, 2001, **73**, 33.
25. B.G.A. Brito, G.-Q. Hai, J.N.T. Rabelo and L. Cândido *Phys. Chem. Chem. Phys.*, 2014, **16**,8639.
26. L. Cândido, J.N.T. Rabelo, J.F. da Silva and G.-Q. Hai, *Phys. Rev. B*, 2012, **85**, 245404.
27. R. J. Needs, M. D. Towler, N. D. Drummond, and P. L. Ríos, *J. Phys.: Condens. Matter*, 2010, **22**, 023201.
28. D. M. Ceperley and B. J. Alder, *Phys. Rev. Lett.*, 1980, **45**, 566.
29. D.J. Feller, *J. Comp. Chem.*, 1996 **17**, 1571; K.L. Schuchardt, B.T. Didier, T. Elsethagen, L. Sun, V. Gurumoorthi, J. Chase, J. Li and T.L. Windus,
30. M. J. Frisch *et al.*, *Gaussian 03, Revision C.02*, Gaussian, Inc., Wallingfort CT, (2004). *J. Chem. Inf. Model.*, 2007, **47**, 1045.
31. N.D. Drummond, M.D. Towler and R.J. Needs, *Phys. Rev. B*, 2004, **70**, 235119.
32. C.J. Umrigar, K.G. Wilson and J.W. Wilkins, *Phys. Rev. Lett.*, 1988, **60**, 1719.
33. N.D. Drummond and R.J. Needs, *Phys. Rev. B*, 2005, **72**, 085124.
34. P.R.C. Kent, R.J. Needs and G. Rajagopal, *Phys. Rev. B*, 1999, **59** 12344.
35. J.R. Trail and R.J Needs, *J. Chem. Phys.*, 2005, **122**, 014112.
36. J.R. Trail and R.J. Needs, *J. Chem. Phys.*, 2005, **122**, 174109.
37. E.L. Shirley and R.M. Martin, *Phys. Rev. B*, 1993, **47**, 15313.
38. J.B. Anderson, *J. Chem. Phys.*, 1975, **65**, 4121.
39. P.J. Reynolds, D.M. Ceperley, B.J. Alder, and W. A. Lester Jr., *J. Chem. Phys.*, 1982, **77**, 5593.
40. A.W. Overhauser *Anomalous effects in simple metals*, John Wiley & Sons,

41. D.M. Ceperley and B.J. Alder, *J. Chem. Phys.*, 1984, **81**, 5833. Edition 4, (2011).

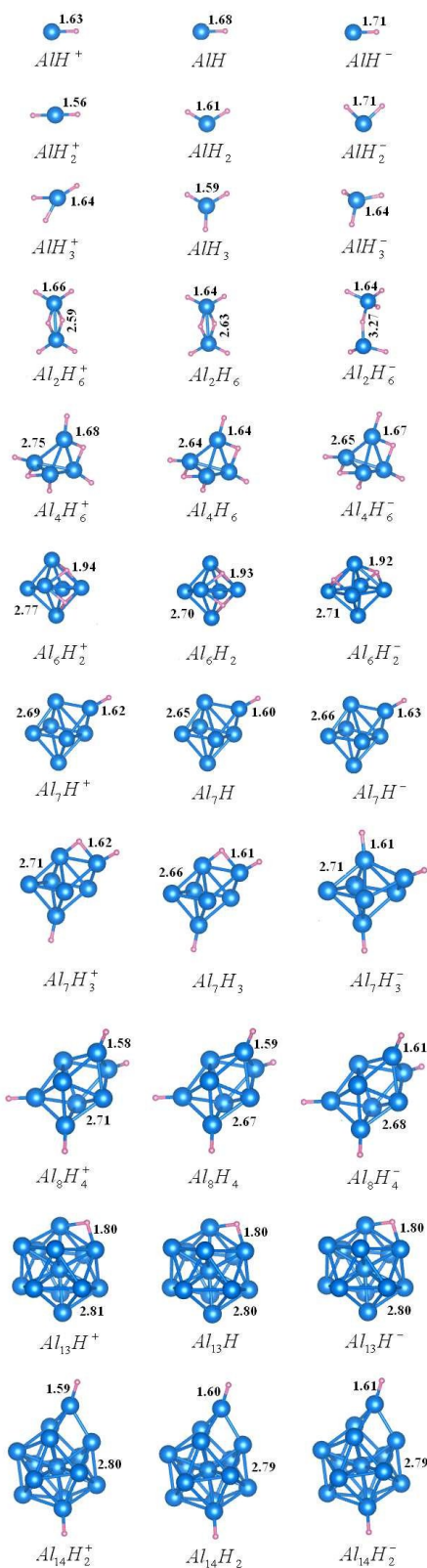


Figure 1: Optimized structures of the Al_nH_m : cationic (left column), neutral (middle), and anionic (right) clusters. The numbers are the main bond lengths in Å.

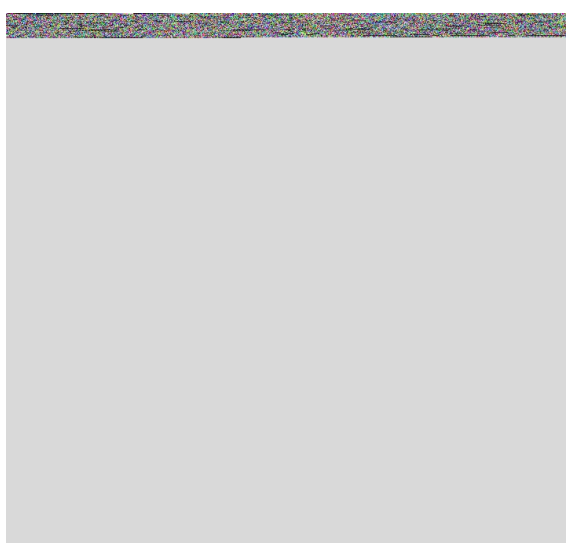


Figure 2: The correlation energy per electron of the neutral, anionic, and cationic Al_nH_m versus the cluster size.